Available online at www.sciencedirect.com
SCIENCE DIRECT®
Journal of Magnetic Resonance 174 (2005) 229–236
JMR Journal of Magnetic Resonance
www.elsevier.com/locate/jmr

Convection-compensating diffusion experiments with phase-sensitive double-quantum filtering

Konstantin I. Momot *, Philip W. Kuchel

School of Molecular and Microbial Biosciences, University of Sydney, Sydney, NSW 2006, Australia

Received 3 November 2004; revised 25 January 2005
Available online 10 March 2005

Abstract

We present a design scheme for phase-sensitive, convection-compensating diffusion experiments with gradient-selected homonuclear double-quantum filtering. The scheme consists of three blocks: a $1/2J$ evolution period during which antiphase single-quantum coherences are created; a period of double-quantum evolution; and another $1/2J$ period, during which antiphase single-quantum coherences are converted back into an in-phase state. A single coherence transfer pathway is selected using an asymmetric set of gradient pulses, and both diffusion sensitization and convection compensation are built into the gradient coherence transfer pathway selection. Double-quantum filtering can be used either for solvent suppression or spectral editing, and we demonstrate examples of both applications. The new experiment performs well in the absence of a field-frequency lock and does not require magnitude Fourier transformation. The proposed scheme may offer advantages in diffusion measurements of spectrally crowded systems, particularly small molecules solubilized in colloidal solutions or bound to macromolecules.

Keywords: Solvent suppression; Convection-compensating NMR diffusion measurements; Gradient coherence transfer pathway selection; DOSY; Drug binding; Drug delivery

1. Introduction

Pulsed-field gradient (PFG)[1] NMR is a highly versatile method for measuring molecular transport and diffusion [1], which is in large part due to the ability to tailor NMR pulse sequences to specific experimental needs. For example, the measurement of molecular diffusion coefficients at high temperatures and/or in low-viscosity solvents requires the elimination of the effects of thermal convection inevitably present under these conditions; this is usually achieved by using convection-compensating NMR diffusion experiments [1–3]. Solvent suppression is another feature commonly desired of NMR diffusion measurements [4–7]. We recently proposed a diffusion experiment (CONVEX) which contains both convection compensation and built-in solvent suppression [4]. In this work, we present another diffusion experiment which contains both these features; but unlike CONVEX, solvent suppression in the present experiment is based on gradient-selected double-quantum filtering. We refer to the new experiment as "DQDiff," for "double-quantum diffusion."

Multiple-quantum (MQ) filtering has long been a useful element in the toolkit of NMR diffusion measurements. Its applications include elimination of dipolar couplings [8,9] and evaluation of the orientational order in liquid-crystalline systems [10–12]; heteronuclear editing of diffusion spectra [13,14]; and as a general way of

* Corresponding author. Fax: +61 2 9351 4726.
E-mail address: konstantin@usyd.edu.au (K.I. Momot).

[1] *Abbreviations used:* CTP, coherence transfer pathway; DDF, dipolar demagnetizing field; DQ(F), double-quantum (filtered); MQ(F), multiple-quantum (filtered); PBS, phosphate-buffered saline; PFG, pulsed-field gradient; (PG)SE, (pulsed-field gradient) spin echo; PGSEcc, convection-compensating double PGSE; RD, radiation damping; SQ, single-quantum.

1090-7807/$ - see front matter © 2005 Elsevier Inc. All rights reserved.
doi:10.1016/j.jmr.2005.02.003

amplifying the effective strength of magnetic field gradients [8,9,15]. In designing the DQDiff experiment, we have set out to incorporate MQ-filtered editing into a convection-compensating diffusion measurement. As will become apparent from the following discussion, the main challenge stemmed from the fact that the stability requirements imposed on MQF schemes appear to be stricter in quantitative diffusion measurements than in general NMR spectroscopy.

Multiple-quantum filtering can be achieved by means of either phase cycling or gradient coherence selection [16–19]. The former method is dependent on the successful cancellation of unwanted signal components and is therefore susceptible to temporal instabilities of the spectrometer, which are usually attributed to transient temperature fluctuations or AC interference [20,21]. In gradient-selected MQ filtering, unwanted signal components are suppressed by means of dephasing, and coherence transfer pathway (CTP) selection does not depend on their cancellation between successive transients. Gradient coherence selection is therefore regarded as a "cleaner" way of MQ filtering; it also enables the selection of a single CTP where phase-cycled selection may not afford it.

2. The DQDiff scheme

The proposed experiment, which is shown in Fig. 1, is actually a family of diffusion experiments which provide solvent suppression by means of gradient-selected double-quantum filtering through a single CTP. CTP selection is governed by the condition

$$\sum_{i=1}^{6} p_i g_i = 0, \tag{1}$$

where the meaning of p_i and g_i is evident from Fig. 1, and normally $p_6 = -1$. The gradients used for coherence selection are the same gradients as used for measuring the diffusion displacement. They can (but need not) be chosen so as to allow for compensation of convection, as discussed below. The number of gradient combinations which select a given CTP and at the same time enable convection compensation is probably infinite, but in practice limited by the quantitative efficiency of dephasing of the unwanted components. Some of the possible sets are shown in Table 1.

The proposed experiment contains a double-quantum evolution period sandwiched between two $1/2J$ periods:

$$I_{\pm} \overset{1/2J}{\rightarrow} I_{\pm}S_z \mid \overset{\pi/2}{\rightarrow} I_{\pm}S_{\pm} \xrightarrow{\text{DQ evolution}} \overset{\pi/2}{\rightarrow} \mid I_{\pm}S_z \overset{1/2J}{\rightarrow} I_{\pm},$$

where I is the observed spin coupled to a like spin S with the coupling constant J. In-phase SQ coherences are converted into antiphase during the first $1/2J$ period, and vice versa during the second. To provide for the refocusing of the chemical shifts, each of the three periods is split in half by a π-pulse, as shown in Fig. 1.

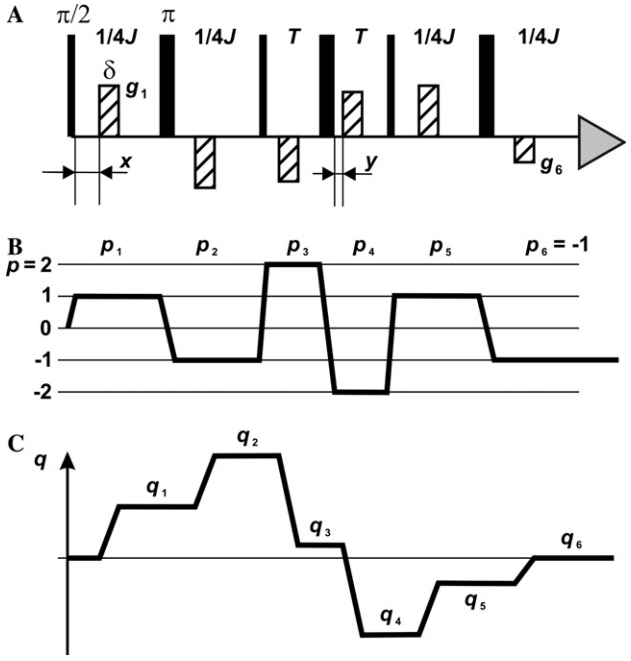

Fig. 1. (A) DQDiff pulse sequence. The gradient values shown here are one of many possible sets which select the CTP $(1,-1,2,-2,1,-1)$; examples of other allowed sets are shown in Table 1. (B) Coherence transfer pathway selected by the pulsed-field gradients. No phase cycling is required for CTP selection. (C) Time dependence of the diffusion wave vector $\mathbf{q}$ defined in Eq. (3). Convection compensation is achieved by adjusting the positions of the gradient pulses (x and y) according to Eq. (8); the gradient set used must allow for this.

The structure of DQDiff is similar to a recently proposed uniform-sign cross-peak DQF COSY experiment [22]. Both experiments create an antiphase state, apply a DQ filter, and then convert the antiphase SQ coherence into an in-phase signal at the beginning of acquisition. A key feature of DQDiff is the asymmetric amplitudes of the gradient pulses. This, in turn, is similar to another DQF COSY experiment where asymmetric gradient values are used to filter out longitudinal interference [23,24]. The selection of a single CTP is inherent in the DQDiff experiment and required by its (CTP-specific) convection compensation [4,25].

The diffusion attenuation of the NMR signal arising from a CTP selected in the sense of Eq. (1) can be calculated using the standard approach:

$$S(q) = S(0)\exp\left\{-D\int_0^{t_s} q^2(t)\,\mathrm{d}t\right\}, \tag{2}$$

where

$$q(t) = \int_0^t \gamma p(t')g(t')\,\mathrm{d}t' \tag{3}$$

and D is the diffusion coefficient of the measured species; γ is the magnetogyric ratio; t_s is the duration of the pulse

Table 1
Examples of gradient combinations selecting the CTP $(1,-1,2,-2,1,-1)$

Relative amplitudes $g_1 : g_2 : g_3 : g_4 : g_5 : g_6$	Convection compensation?	Other selected CTPs?	Suitable?
8 : −8 : −7 : 7 : 8 : −4	Yes	None	Yes; "best" gradient set
5 : 7 : −8 : 3 : 7 : −3	Yes	None	Yes, but less resistant to second-order leaks
7 : 7 : −5 : −7 : −5 : −1	Yes	−1, 1, 2, −2, 1, −1	No: only one CTP is convection-compensated
1 : −7 : −3 : −5 : −7 : 5	No	None	Not suitable when convection is present

sequence from the first RF excitation pulse to the beginning of acquisition; g is the field gradient amplitude; and p is the coherence order [4]. For a coherence transfer pathway $(p_1,p_2,p_3,p_4,p_5,-1)$ which satisfies Eq. (1), g_6 can be expressed as $p_1g_1+p_2g_2+p_3g_3+p_4g_4+p_5g_5$. Integration of Eq. (2) with rectangular gradient pulses then produces

$$S(g) = S(0)\,\mathrm{e}^{-D\gamma^2g^2\delta^2(PU+QT+Vx+Wy+R\delta)}, \tag{4}$$

where U is ideally set to $1/4J$; T, δ, x, and y are shown in Fig. 1; the unitless quantities P, Q, R, V, and W are given by

$$\begin{aligned}
P &= \left(\sum_{i=2}^{5} c_ip_i\right)^2 + (c_1p_1+c_2p_2)^2 + 2c_1p_1\sum_{i=1}^{5} c_ip_i,\\
Q &= 2\left(\sum_{i=1}^{3} c_ip_i\right)^2 + c_4p_4(2c_1p_1+2c_2p_2+2c_3p_3+c_4p_4),\\
V &= -W = (c_3p_3+c_4p_4)(2c_1p_1+2c_2p_2+c_3p_3+c_4p_4),\\
R &= -\frac{1}{3}\sum_{i=j}^{5}\sum_{j=1}^{5} c_ip_ic_jp_j,
\end{aligned} \tag{5}$$

and $g_i = c_ig$. For trapezoidal gradient pulses with the ramp time τ, Eq. (2) becomes

$$S(g) = S(0)\,\exp\left\{-D\gamma^2g^2\left[\delta^2(PU+QT+Vx+Wy) + R\left(\delta^3+\frac{\delta\tau^2}{2}-\frac{\tau^3}{10}\right)\right]\right\}. \tag{6}$$

Eqs. (4)–(6) contain no assumptions about convection compensation. While they are somewhat cumbersome, their form is fundamentally no different from the simple PGSE experiment [1], and the plots of $\ln(S)$ vs q^2 (Stejskal–Tanner plots) are linear with the slope proportional to $-D$.

Convection (or, to be precise, local velocity) compensation is given by the condition

$$\int_0^{t_s} q(t)\,\mathrm{d}t = 0. \tag{7}$$

In addition to the appropriate choice of the amplitudes, gradient pulses need to be correctly positioned relative to the RF pulses to satisfy Eq. (7). For a given CTP, the values $\mathbf{q}_1-\mathbf{q}_6$ in Fig. 1 depend only on the areas of the gradients, not on x or y. When $\mathbf{q}$ is integrated over time, the resulting expression is therefore linear in both x and y. The easiest way to achieve convection compensation (CC) is then to choose an arbitrary, small y, and solve Eq. (7) for x. For the CTP $(p_1,p_2,p_3,p_4,p_5,-1)$, the result (which is unique but not always physically meaningful) is given by

$$\begin{aligned}
x_{\mathrm{CC}} = &-\frac{3c_1p_1+2c_2p_2+c_3p_3+c_4p_4+c_5p_5}{c_3p_3+c_4p_4}U\\
&-\frac{2c_1p_1+2c_2p_2+2c_3p_3+c_4p_4}{c_3p_3+c_4p_4}T+y.
\end{aligned} \tag{8}$$

This assumes that the CTP in question satisfies Eq. (1); by definition, convection-compensating sets of gradient pulses are those for which $0 < x_{\mathrm{CC}} < 1/4J$. Fig. 1 shows one of many gradient combinations which are capable of providing for convection compensation of the CTP $(1,-1,2,-2,1,-1)$.

3. Materials and methods

3.1. Sample preparation

Reagents were purchased from the following sources: propofol, from Archimica SpA (Varese, Italy); Solutol HS15, from BASF (Ludwigshafen, Germany); lysozyme, from Sigma (St. Louis, MO); chloroform, from APS (Seven Hills, NSW, Australia); carbon tetrachloride (spectroscopic grade), from AJAX Chemicals (Auburn, NSW, Australia). All chemicals were used as received. Water was obtained from a Milli-Q reverse-osmosis apparatus (Millipore, Bedford, MA). The micellar solution of propofol [1%(w/w) propofol/10%(w/w) Solutol HS15/D_2O-saline] was prepared as described previously [26]. 1.5 mM lysozyme in phosphate-buffered saline [PBS; pH 6.5; 10 mM total phosphate ($K_2HPO_4 + KH_2PO_4$); NaCl added to osmolality 289 ± 2 mM] was prepared as described previously [4].

3.2. NMR setup and measurements

All measurements were carried out on a Bruker DRX-400 wide-bore NMR spectrometer equipped with a 1000 G cm^{-1} z-only actively shielded diffusion probe; the general setup has been described previously [4,26,27]. The propofol/$CHCl_3$ sample was studied in a 5-mm D_2O-matched Shigemi tube (Allison Park, PA).

The lysozyme/water and propofol/Solutol/D_2O samples were studied in a cylindrical Wilmad microcell (Buena, NJ) inserted into a 10-mm NMR tube filled with CCl_4 for magnetic susceptibility matching. In either case, the length of the sample was constrained to 8–9 mm in order to contain it within the constant-gradient region of the probe. All measurements used trapezoidal gradient pulses with 0.1-ms ramp times; typical pulse duration was 1 or 2 ms; no lock was used. Measurements were performed with a detuned probe in order to alleviate radiation damping (RD), except where the evaluation of RD effects was specifically sought. Typical duration of the 90° pulse was 20 and 34 μs for the tuned and the detuned diffusion probe, respectively. NMR data were processed, and the diffusion coefficients determined, as described previously [4,26–28]. Phase correction of diffusion spectra was uniform within any given experimental set, and no baseline correction of the spectra was used. Stejskal–Tanner plots were processed according to Eq. (6).

4. Results

The diffusion coefficient of propofol in two solutions was measured: (1) a 3.16%(w/w) solution in non-deuterated chloroform and (2) a 1%(w/w) micellar solution in 10% Solutol HS15/D_2O-saline. The ^1H NMR spectrum of each system is shown in Fig. 2. Representative Stejskal–Tanner plots are shown in Fig. 3. The choice of these systems was determined by the fact that in each of them some of the propofol peaks (marked with the arrows in Fig. 2) are either in the vicinity of relatively large peaks or obscured by other peaks. An accurate determination of the diffusion coefficient requires not only spectral resolution but also phase stability of the large peaks. The respective peaks have comparable diffusion coefficients; therefore, Stejskal–Tanner resolution cannot be achieved by merely shifting the window of the q values. All this provides for a challenging performance test of the DQDiff experiment. The other factor determining the choice of the test systems was that both of them resemble systems of "practical" interest which might be studied in colloidal or pharmaceutical chemistry; in fact, the solution of propofol in Solutol/D_2O-saline was the subject of an earlier investigation as a potential drug delivery system [26]. The diffusion coefficients determined by different methods from different propofol peaks are presented in Tables 2 and 3. For PGSE measurements in Table 2, D was determined from the initial decay, disregarding the presence of convection-induced oscillations.

We have also attempted the measurement of the diffusion coefficient of lysozyme in PBS [4,29]. This measurement was unsuccessful due to the short ^1H transverse relaxation times in the protein, and no numerical results are presented here.

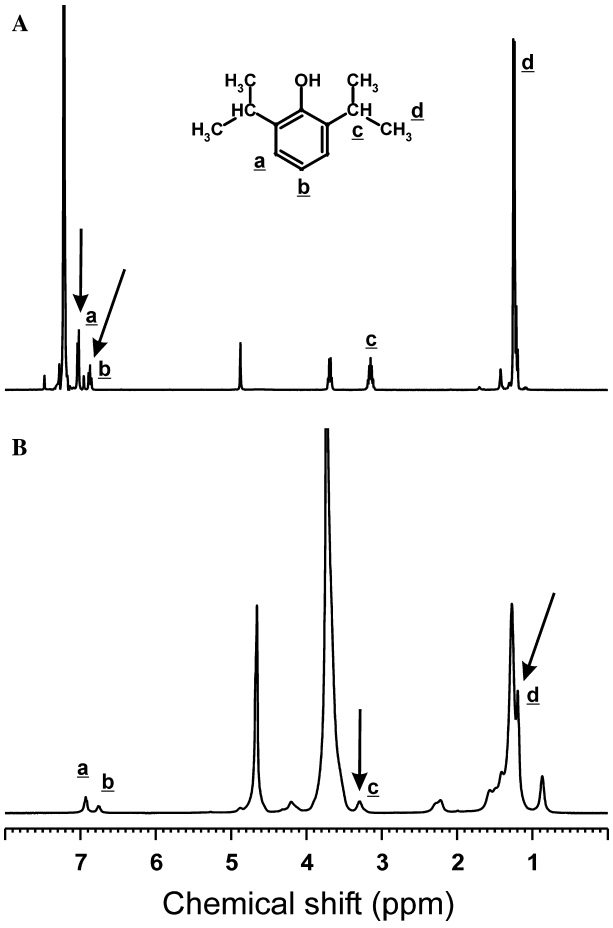

Fig. 2. NMR spectra of the two test systems used in this work: (A) 3.16%(w/w) propofol in $CHCl_3$; (B) 1%(w/w) propofol and 10%(w/w) Solutol HS15 in D_2O-saline. Propofol peaks are marked a through d [26]. The other peaks are H_2O (1.43 ppm), acetone (4.88 ppm), and ethanol (1.22, 3.69 ppm) impurities; chloroform (7.22 ppm) in (A); HDO (4.67 ppm) and Solutol HS15 (multiple peaks between 0.8 and 4.2 ppm) in (B). Propofol peaks marked with arrows are those which present particular challenges to the measurement of the diffusion coefficient due to their proximity to other peaks.

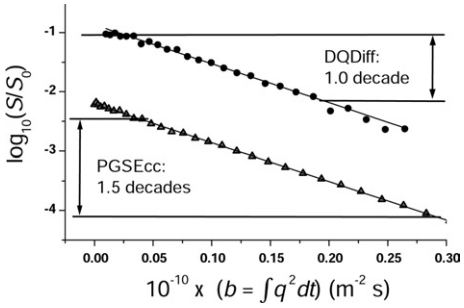

Fig. 3. A representative Stejskal–Tanner plot from a DQDiff measurement (propofol in $CHCl_3$; peak a of Table 2 and Fig. 2A was used for this plot). The lower data set was uniformly displaced down by −2 for clarity.

5. Discussion

While MQF solvent suppression methods are plentiful in general NMR spectroscopy [18,30], our experience

Table 2
Diffusion coefficients of propofol in $CHCl_3$ at 38.4 ± 0.5 °C measured by different ^1H NMR methods

Measurement	Proton	D ($m^2 s^{-1}$)	Linear range
PGSE $\Delta = 5$ ms	a	$(3.09 \pm 0.04) \times 10^{-9}$	1.3
	b	$(3.01 \pm 0.05) \times 10^{-9}$	1.2
	c	$(3.20 \pm 0.02) \times 10^{-9}$	1.3
	d	$(3.43 \pm 0.02) \times 10^{-9}$	1.4
PGSE $\Delta = 10$ ms	a	$(4.6 \pm 0.1) \times 10^{-9}$	0.8
	b	$(4.2 \pm 0.3) \times 10^{-9}$	0.6
	c	$(4.98 \pm 0.04) \times 10^{-9}$	0.7
	d	$(5.36 \pm 0.03) \times 10^{-9}$	0.9
PGSEcc $\Delta = 5$ ms	a	$(1.50 \pm 0.01) \times 10^{-9}$	1.5
	b	$(1.49 \pm 0.02) \times 10^{-9}$	1.4
	c	$(1.40 \pm 0.01) \times 10^{-9}$	1.4
	d	$(1.53 \pm 0.01) \times 10^{-9}$	2.1
CONVEX	a	Suppressed	0
$\Delta_1 = 5$ ms, $C = 5/7$	b	Suppressed	0
	c	$(1.54 \pm 0.01) \times 10^{-9}$	1.2
	d	$(1.53 \pm 0.01) \times 10^{-9}$	2.7
DQDiff 8 : 8 :	a	$(1.52 \pm 0.03) \times 10^{9}$	1.0
−7 : 7 : 8 : −4	b	$(1.51 \pm 0.03) \times 10^{-9}$	1.3
	c	$(1.61 \pm 0.05) \times 10^{-9}$	1.1
	d	$(1.51 \pm 0.02) \times 10^{-9}$	1.6

The four values in each cell refer to the four propofol multiplets (see Fig. 2). "Linear range" is the $\log_{10}$ vertical span of the Stejskal–Tanner region in which signal attenuation was linear [4]. PGSEcc is convection-compensating double PGSE [2], and CONVEX is convection-compensating double PGSE with excitation-sculpting solvent suppression [4].

Table 3
Diffusion coefficients of propofol in 10%(w/w) Solutol HS15/D_2O-saline at 38.0 ± 0.5 °C measured by different ^1H NMR methods

Measurement	Proton	D ($m^2 s^{-1}$)	Linear range
PGSEcc $\Delta = 6$ ms	a	$(2.13 \pm 0.02) \times 10^{-11}$	1.3
	b	$(1.88 \pm 0.02) \times 10^{-11}$	1.0
	c	Unresolved	0
	d	Unresolved	0
PGSEcc $\Delta = 35$ ms	a	$(1.89 \pm 0.01) \times 10^{11}$	1.5
	b	$(2.07 \pm 0.03) \times 10^{-11}$	1.2
	c	$(1.92 \pm 0.04) \times 10^{-11}$	2.1
	d	$(1.97 \pm 0.01) \times 10^{-11}$	2.2
DQDiff 8 : −8 :	a	$(1.96 \pm 0.02) \times 10^{-11}$	1.1
−7 : 7 : 8 : −4	b	$(1.83 \pm 0.03) \times 10^{-11}$	1.1
	c	$(1.94 \pm 0.06) \times 10^{-11}$	0.8
	d	$(1.91 \pm 0.02) \times 10^{11}$	1.1

The four values in each cell refer to the four propofol multiplets (see Fig. 2).

has been that many of the non-echo-based schemes fail to provide the stability required for quantitative diffusion applications. For example, in diffusion measurements based on a three-pulse GS COSY sequence [23] the antiphase signal is prone to partial self-cancellation between transients. While the resulting t_1 noise is not a fatal problem in qualitative COSY experiments [31,32], the variation of points in Stejskal–Tanner plots can be very large. This problem is avoided in the DQDiff scheme in which the acquired signal is in-phase. Another advantage of the DQDiff scheme is that it does not require a magnitude Fourier transform of the FID, thus preserving the zero-average noise and limiting baseline distortions near large signals.

The values of the diffusion coefficient of propofol in $CHCl_3$ determined from double-echo convection-compensating PGSE (PGSEcc [2]) and DQDiff measurements were $(1.48 \pm 0.05) \times 10^{-9}$ and $(1.54 \pm 0.05) \times 10^{-9}$ $m^2 s^{-1}$, respectively. (The standard deviations take into account the errors of the individual measurements.) The respective values for propofol in Solutol/D_2O solution were $(1.96 \pm 0.07) \times 10^{-11}$ and $(1.91 \pm 0.06) \times 10^{-11}$ $m^2 s^{-1}$. Although the ranges of linear Stejskal–Tanner attenuation in PGSEcc measurements exceeded those from DQDiff, the reproducibility and the overall accuracy of DQDiff measurements were the same or marginally better than those in PGSEcc.

5.1. Choice of pulsed-field gradient amplitudes

Pulsed-field gradients in the DQDiff scheme both sensitize the sample to molecular displacement and select the required CTP. The choice of gradient values in the present work is based on the CTP $(1, -1, 2, -2, 1, -1)$. Similar pathways, such as $(-1, 1, 2, -2, 1, -1)$, could also be used, as long as the gradient values are changed accordingly. Whichever CTP is used, asymmetric time dependence of $\mathbf{q}$ makes convection compensation in this scheme CTP-specific. The consequence of this is that the diffusion measurement must be based on a single coherence transfer pathway.

Some candidate gradient sets are easily identified as unsuitable: for example, any set which selects the CTP $(1, -1, 2, -2, 1, -1)$ and has $g_1 = g_2$, is also going to select $(-1, 1, 2, -2, 1, -1)$, and vice versa; therefore, any set with $g_1 = g_2$ is a priori unsuitable. In general, however, a systematic search for candidate gradient sets and the evaluation of their suitability has to involve a type of "throughput screening" of gradient sets against all possible CTPs. This is a computationally voluminous problem which can be reduced by using some algorithmic finesse. Of the ~11 million distinct gradient combinations which are integer-valued between −8 and +8, approximately 250,000 select the target CTP; of these, ~90,000 potentially provide for its convection compensation. The requirement that the target CTP be selected exclusively is the principal factor which limits the number of allowed gradient combinations: only ~500 of the 90,000 candidates satisfy this criterion. The selection can be refined on the basis of two additional criteria: minimization of second-order leaks (i.e., those resulting from imperfectly set RF pulse angles and durations of delays)

and maximization of the dephasing efficiency of unwanted CTPs. The latter reduces the attractiveness of higher-valued integer sets (e.g., $16:-16:-15:8:6:-8$), because in a finite-length sample such gradient sets could fail to sufficiently dephase the non-selected components.

The screening and refinement were done in *Mathematica*, and on a standard desktop PC required ~2–3 days of CPU time. Selected examples of both satisfactory and unsatisfactory gradient combinations are given in Table 1. Clearly, it was not possible to examine experimentally all of the possible combinations; of those that we examined, the set $(8:-8:-7:7:8:-4)$ yielded the best practical results. Other sets may exist, which could provide for a still better performance.

5.2. Convection compensation

Although convection compensation is an optional feature in the DQDiff scheme, it becomes a practical necessity in solutions of viscosity <1 cP. The typical value of $^3J_{HH}$ (~7 Hz) requires that the diffusion-sensitive magnetization helix remains wound for ~100 ms in proton measurements; this could result in significant effects of convection even near room temperature in a typical aqueous or organic solution. For this reason, the DQDiff scheme was always used in convection-compensating mode in this work, except for a few cases that were intended to be an illustration of uncompensated convection effects.

As shown in Eq. (8), convection compensation requires not only the appropriate relative gradient amplitudes, but also the correct positioning of the gradients relative to the RF pulses. The values of x_{CC} can typically range between 10 and 25 ms (assuming $J \sim 7$ Hz, $\delta = 1$ ms, $T \sim 5$ ms, and $y = 0.1$ ms). Interestingly, satisfying the convection-compensation condition eliminates both x and y from the diffusion attenuation expression. Eq. (6) in this case simplifies to

$$S(g) = S(0)\exp\left\{-D\gamma^2 g^2\left[\delta^2(HU+IT) + R\left(\delta^3 + \frac{\delta\tau^2}{2} - \frac{\tau^3}{10}\right)\right]\right\}, \tag{9}$$

where R is given by Eq. (5), and

$$\begin{aligned} H &= -3(c_1p_1 + c_2p_2)^2 - (c_3p_3 + c_4p_4) \\ &\quad \times (3c_1p_1 + 2c_2p_2 - c_5p_5) + c_2^2p_2^2 + c_5^2p_5^2, \\ I &= -2(c_1p_1 + c_2p_2)^2 - 2(c_1p_1 + c_2p_2) \\ &\quad \times (c_3p_3 + c_4p_4) - c_3p_3c_4p_4. \end{aligned} \tag{10}$$

A similar simplification can be invoked for Eq. (4).

A comparison of representative convection-compensated and -uncompensated measurements can be made from the results presented in Table 2. As the diffusion coefficients determined from the two PGSE experiments ($\Delta = 5$ and 10 ms) differ markedly, it is clear that convection compensation was necessary under the conditions involved. This was provided by PGSEcc [2], CONVEX [4], and DQDiff measurements; their comparison reveals that the convection compensation afforded by the DQDiff scheme was sufficient.

5.3. Solvent suppression efficiency

For the propofol/$CHCl_3$ system, we investigated the effect of WaterPress solvent suppression [5] with a selective π pulse inverting the chloroform peak a time $T_1 \ln 2$ prior to the DQDiff sequence. This modification did not result in an improvement in the accuracy of the measured D values; conversely, it produced baseline distortions near the solvent peak and made one of the nearby solute peaks unusable for the determination of D.

The gradient-selected DQDiff solvent suppression was efficient and resulted in the practically complete cancellation of the chloroform peak beyond $q \sim 3\times10^8$ m^{-1}. Some of the points prior to this value needed to be excluded, but the remaining useful range of q was sufficient for the determination of D even from very small peaks less than 80 Hz away from a solvent peak having ~30 times the intensity of the solute (peaks a, b in Table 2). The accuracy of the resulting Stejskal–Tanner fits was even better for the peaks that were well-separated from the solvent (>1000 Hz).

5.4. Macroscopic magnetization effects

As is the case for many NMR experiments involving solvent suppression [5], radiation damping (RD) had a significant deleterious effect on the quality of DQDiff measurements. The example in Fig. 4 illustrates this. The spectrum in Fig. 4A was acquired with a fully tuned TXI probe in order to emphasize RD effects (90° pulse duration 7.4 μs; TXI probe was used in this case only). The strongly radiation-damped solvent signal failed to undergo full cancellation in this case, and the lineshapes of nearby peaks were irretrievably distorted. The spectrum in part B was recorded with a detuned diffusion probe (90° pulse duration 34 μs, no measurable RD effects) and is free of the problems seen in Fig. 4A.

Dipolar demagnetizing field (DDF) can also adversely affect diffusion measurements carried out in protonated solvents. We have no reason to conclude that this was the case in DQDiff measurements, because (1) the use of WaterPress solvent suppression adversely affected the precision of the diffusion coefficients determined from the peaks near solvent, and (2) it did not improve the accuracy of the diffusion coefficients measured from the peaks far away from the solvent. On the other hand, we did not carry out a systematic investigation of

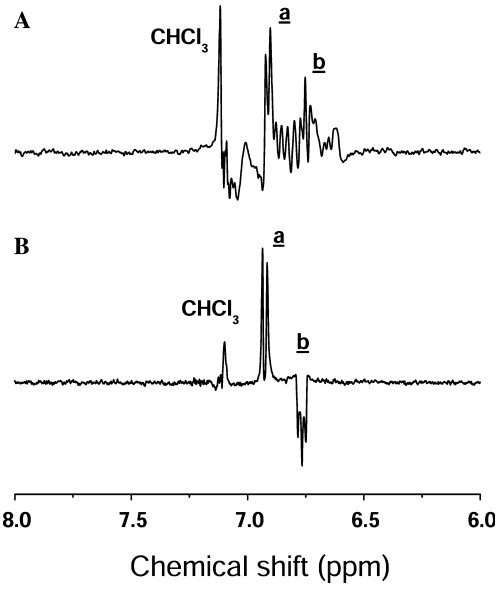

Fig. 4. Effect of radiation damping on DQDiff spectra. Aromatic region of DQDiff spectra of propofol in $CHCl_3$ was recorded with (A) a fully tuned TXI probe and (B) a detuned diffusion probe. In (A), radiation damping reduced the suppression efficiency of the large chloroform peak at 7.22 ppm and severely distorted the nearby propofol peaks. This was remedied by using a detuned probe (see Section 3).

the possible effects of DDF, and it is conceivable that nulling the DDF with magic-angle gradients [5] could be beneficial to the performance of DQDiff.

5.5. Phase cycling

The CTP selection in DQDiff experiments is handled by the pulsed-field gradients, and no phase cycling is required. As a test, we carried out DQDiff measurements of both propofol-containing test systems with the use of Exorcycle on the last π pulse, as well as non-phase-cycled measurements with the same number of transients. The differences between the two methods were marginal and trendless, i.e., the phase cycling neither improved nor reduced the precision of the diffusion plots. A partial phase cycle selecting $\Delta p = \pm 4$ on the second π pulse (RF 0, 1, 2, 3; AQ 0, 0, 0, 0) also did not result in any improvement.

5.6. Other factors

As discussed above, the good performance of DQDiff experiments in the absence of field-frequency lock was in large part due to the fact that phase-sensitive, in-phase spectra were acquired. This prevented signal self-cancellation to which antiphase spectra were prone; and phase-sensitive Fourier transformation minimized baseline distortions. Baseline correction did not result in a measurable improvement in the accuracy of DQDiff-estimated diffusion coefficients. We found DQDiff measurements to be more demanding with respect to gradient blanking and zero-current calibration than either PGSE or PGSEcc measurements. This is probably due to the asymmetric nature of the DQDiff pulse sequence, and was easily remedied by optimizing the blanking and zero-gradient current parameters.

The effects of missetting the durations of RF pulses and the $1/4J$ delay are another factor to consider. The effects of moderately (5–10%) misset RF pulse lengths were negligible, and the effects of missetting $1/4J$ were negligible for peaks of low multiplicity. However, peaks of large multiplicity (e.g., propofol septet at 3.3 ppm, peak c in Fig. 2) exhibited a baseline that was concave upwards when the $1/4J$ delay durations were misset by 10–15%. As is evident from Table 2, this had an adverse effect on the precision of integration of this peak and the estimate of the diffusion coefficient. Unfortunately, there does not seem to be an obvious way around this limitation. As the in-phase component I_z reappears as $\cos^n(Jt)$ under scalar-coupled evolution in the IS_n system, a larger n leaves less room for the variation of $U = 1/4J$. For this reason, MQF diffusion experiments based on large coherence orders ($p > 4$) could be impractical as an alternative to DQ filtering.

The main drawback of the DQDiff scheme appears to be its high cost in terms of S:N ratio. The selection of a single CTP means that even in the ideal situation the amplitude of the acquired signal is only 25% of that available in the PGSEcc experiment. Imperfection in the setting of delay and pulse lengths brings about further losses, as does transverse relaxation. Signal loss due to the latter can be very significant for large molecules, as attested to by our failure to observe readily a DQDiff spectrum of lysozyme. Because the magnetization remains in the transverse plane for $\sim 1/J$ (i.e., ~140 ms for a typical $^3J_{HH}$), in practice the method is limited to small- to medium-sized molecules with $T_2 > 100$ ms.

6. Conclusions

The proposed DQDiff scheme is a useful new method for measuring diffusion coefficients of small- or medium-sized solutes in non-deuterated solvents or in spectrally crowded systems. Although it does not appear to offer an across-the-board improvement over the existing convection-compensating methods, and CONVEX remains our method of choice for most situations requiring solvent suppression, DQDiff provides a potential advantage when small scalar-coupled solute peaks are directly covered by large peaks with no homonuclear couplings. Examples of the latter are peaks belonging to a solvent or (in the case of colloidal systems) a surfactant. The method may also be beneficial for measuring the diffusion of small molecules bound to macromolecules, i.e., a small-molecule drug bound to a protein.

Acknowledgments

This work was supported by an ARC-SPIRT grant to P.W.K. and K.I.M. and an ARC discovery grant to P.W.K. We thank Dr. Saad Ramadan for fruitful discussions; Professor Bill Price and Dr. Claudio Dalvit for copies of the reviews [5,30], respectively; Mr. Bill Lowe for technical assistance; and Drs. Bill Bubb and Bob Chapman for NMR spectroscopic assistance.

References

[1] C.S. Johnson, Diffusion ordered nuclear magnetic resonance spectroscopy: principles and applications, Prog. Nucl. Magn. Reson. Spectrosc. 34 (1999) 203–256.
[2] G.H. Sørland, J.G. Seland, J. Krane, H.W. Anthonsen, Improved convection compensating pulsed field gradient spin-echo and stimulated-echo methods, J. Magn. Reson. 142 (2000) 323–325.
[3] A. Jerschow, N. Müller, Suppression of convection artifacts in stimulated-echo diffusion experiments. Double-stimulated-echo experiments, J. Magn. Reson. 125 (1997) 372–375.
[4] K.I. Momot, P.W. Kuchel, Convection-compensating PGSE experiment incorporating excitation-sculpting water suppression (CONVEX), J. Magn. Reson. 169 (2004) 92–101.
[5] W.S. Price, Water signal suppression in NMR spectroscopy, Annu. Rep. NMR Spectrosc. 38 (1999) 289–354.
[6] W.S. Price, F. Elwinger, C. Vigouroux, P. Stilbs, PGSE-WATERGATE, a new tool for NMR diffusion-based studies of ligand-macromolecule binding, Magn. Reson. Chem. 40 (2002) 391–395.
[7] C. Dalvit, J.M. Bohlen, Analysis of biofluids and chemical mixtures in non-deuterated solvents with ^{1}H diffusion-weighted PFG phase-sensitive double-quantum NMR spectroscopy, NMR Biomed. 10 (1997) 285–291.
[8] J.F. Martin, L.S. Selwyn, R.R. Vold, R.L. Vold, The determination of translational diffusion constants in liquid crystals from pulsed field gradient double quantum spin echo decays, J. Chem. Phys. 76 (1982) 2632–2634.
[9] D. Zax, A. Pines, Study of anisotropic diffusion of oriented molecules by multiple quantum spin echoes, J. Chem. Phys. 78 (1983) 6333–6334.
[10] L.D. Field, S.A. Ramadan, G.K. Pierens, Multiple-quantum NMR spectra of partially oriented indene: a new approach to estimating order in a nematic phase, J. Magn. Reson. 156 (2002) 64–71.
[11] S.A. Ramadan, L.D. Field, G.K. Pierens, Multiple quantum nuclear magnetic resonance spectra of partially oriented styrene in a nematic phase, Mol. Phys. 101 (2003) 1813–1818.
[12] L.D. Field, S.A. Ramadan, Multiple quantum NMR spectra of toluene and *p*-bromotoluene partially aligned in a nematic phase, Magn. Reson. Chem. 41 (2003) 933–938.
[13] P.W. Kuchel, B.E. Chapman, Heteronuclear double-quantum-coherence selection with magnetic-field gradients in diffusion experiments, J. Magn. Reson. A 101 (1993) 53–59.
[14] B.E. Chapman, P.W. Kuchel, Sensitivity in heteronuclear multiple-quantum diffusion experiments, J. Magn. Reson. A 102 (1993) 105–109.
[15] M. Liu, X.-A. Mao, C. Ye, J.K. Nicholson, J.C. Lindon, Enhanced effect of magnetic field gradients using multiple quantum NMR spectroscopy applied to self-diffusion coefficient measurement, Mol. Phys. 93 (1998) 913–920.
[16] M.H. Levitt, Spin Dynamics: Basics of Nuclear Magnetic Resonance, Wiley, Chichester, 2001.
[17] R.R. Ernst, G. Bodenhausen, A. Wokaun, Principles of Nuclear Magnetic Resonance in One and Two Dimensions, Clarendon Press, Oxford, 1987.
[18] T.J. Norwood, Multiple-quantum NMR methods, Prog. Nucl. Magn. Reson. Spectrosc. 24 (1992) 295–375.
[19] C.E. Hughes, M. Carravetta, M.H. Levitt, Some conjectures for cogwheel phase cycling, J. Magn. Reson. 167 (2004) 259–265.
[20] G.A. Morris, Systematic sources of signal irreproducibility and t_1 noise in high-field NMR spectrometers, J. Magn. Reson. 100 (1992) 316–328.
[21] P.J. Bowyer, A.G. Swanson, G.A. Morris, Analyzing and correcting spectrometer temperature sensitivity, J. Magn. Reson. 152 (2001) 234–246.
[22] L.J. Mueller, D.W. Elliott, G.M. Leskowitz, J. Struppe, R.A. Olsen, K.-C. Kim, C.A. Reed, Uniform-sign cross-peak double-quantum-filtered correlation spectroscopy, J. Magn. Reson. 168 (2004) 327–335.
[23] A.A. Shaw, C. Salaun, J.F. Dauphin, B. Ancian, Artifact-free PFG-enhanced double-quantum-filtered COSY experiments, J. Magn. Reson. A 120 (1996) 110–115.
[24] B. Ancian, I. Bourgeois, J.F. Dauphin, A.A. Shaw, Artifact-free pure absorption PFG-enhanced DQF-COSY spectra including a gradient pulse in the evolution period, J. Magn. Reson. 125 (1997) 348–354.
[25] A. Jerschow, N. Müller, Convection compensation in gradient enhanced nuclear magnetic resonance spectroscopy, J. Magn. Reson. 132 (1998) 13–18.
[26] K.I. Momot, P.W. Kuchel, B.E. Chapman, P. Deo, D. Whittaker, NMR study of the association of propofol with nonionic surfactants, Langmuir 19 (2003) 2088–2095.
[27] K.I. Momot, P.W. Kuchel, D. Whittaker, Enhancement of Na^{+} diffusion in a bicontinuous cubic phase by the ionophore monensin, Langmuir 20 (2004) 2660–2666.
[28] K.I. Momot, P.W. Kuchel, Pulsed field gradient nuclear magnetic resonance as a tool for studying drug delivery systems, Concepts Magn. Reson. A 19 (2003) 51–64.
[29] W.S. Price, F. Tsuchiya, Y. Arata, Lysozyme aggregation and solution properties studied using PGSE NMR diffusion measurements, J. Am. Chem. Soc. 121 (1999) 11503–11512.
[30] C. Dalvit, J.M. Bohlen, Proton phase-sensitive pulsed field gradient double-quantum spectroscopy, Annu. Rep. NMR Spectrosc. 37 (1999) 203–271.
[31] A.D. Bain, I.W. Burton, W.F. Reynolds, Artifacts in 2-dimensional NMR, Prog. Nucl. Magn. Reson. Spectrosc. 26 (1994) 59–89.
[32] P.J. Bowyer, A.G. Swanson, G.A. Morris, Randomized acquisition for the suppression of systematic F_1 artifacts in two-dimensional NMR spectroscopy, J. Magn. Reson. 140 (1999) 513–515.